Supplementary Information for

De novo germline mutation in the dual specificity phosphatase 10 gene accelerates autoimmune diabetes

Anne-Perrine Foray, Sophie Candon, Sara Hildebrand, Cindy Marquet, Fabrice Valette, Coralie Pecquet, Sebastien Lemoine, Francina Langa-Vives, Michael Dumas, Peipei Hu, Père Santamaria, Sylvaine You, Stephen Lyon, Lindsay Scott, Chun Hui Bu, Tao Wang, Darui Xu, Eva Marie Y. Moresco, Claudio Scazzocchio, Jean-François Bach*, Bruce Beutler*, Lucienne Chatenoud*
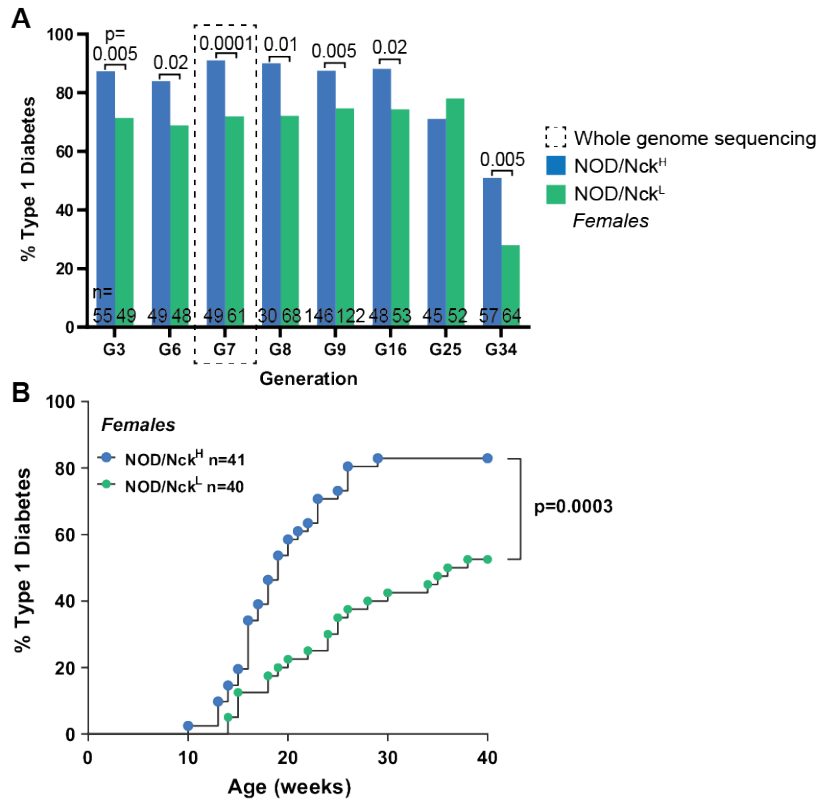
Correspondence to: Jean-François Bach, jean-francois.bach@academie-sciences.fr;
Bruce Beutler, Bruce.Beutler@UTSouthwestern.edu;
Lucienne Chatenoud, lucienne.chatenoud@inserm.fr.

This PDF file includes:

> Figures S1 to S9
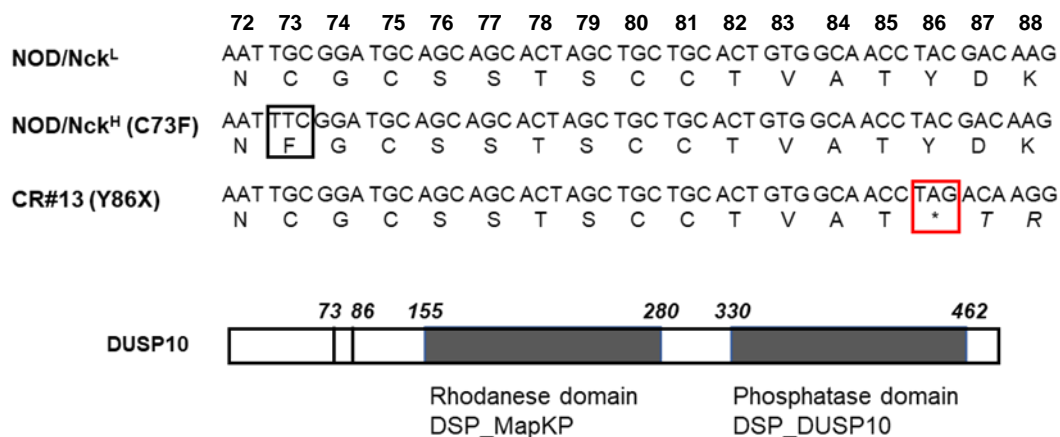> Table S1
> Legend for Dataset S1
> SI References 1-9

Other Supplementary Information for this manuscript include the following:

> Dataset S1

Fig. S1.
Diabetes incidence in female sublines of the NOD/Nck strain. (**A**) Incidence of T1D in NOD/Nck[H] and NOD/Nck[L] female mice from generation 3 up to generation 34. (**B**) Incidence of T1D in NOD/Nck[H] and NOD/Nck[L] female mice derived from embryos frozen at generation 7 and revitalized.

| | 72 | 73 | 74 | 75 | 76 | 77 | 78 | 79 | 80 | 81 | 82 | 83 | 84 | 85 | 86 | 87 | 88 |

NOD/Nck^L
AAT TGC GGA TGC AGC AGC ACT AGC TGC TGC ACT GTG GCA ACC TAC GAC AAG
N   C   G   C   S   S   T   S   C   C   T   V   A   T   Y   D   K

NOD/Nck^H (C73F)
AAT TTC GGA TGC AGC AGC ACT AGC TGC TGC ACT GTG GCA ACC TAC GAC AAG
N   F   G   C   S   S   T   S   C   C   T   V   A   T   Y   D   K

CR#13 (Y86X)
AAT TGC GGA TGC AGC AGC ACT AGC TGC TGC ACT GTG GCA ACC TAG ACA AGG
N   C   G   C   S   S   T   S   C   C   T   V   A   T   *   T   R

DUSP10
73 86   155   280   330   462
Rhodanese domain   Phosphatase domain
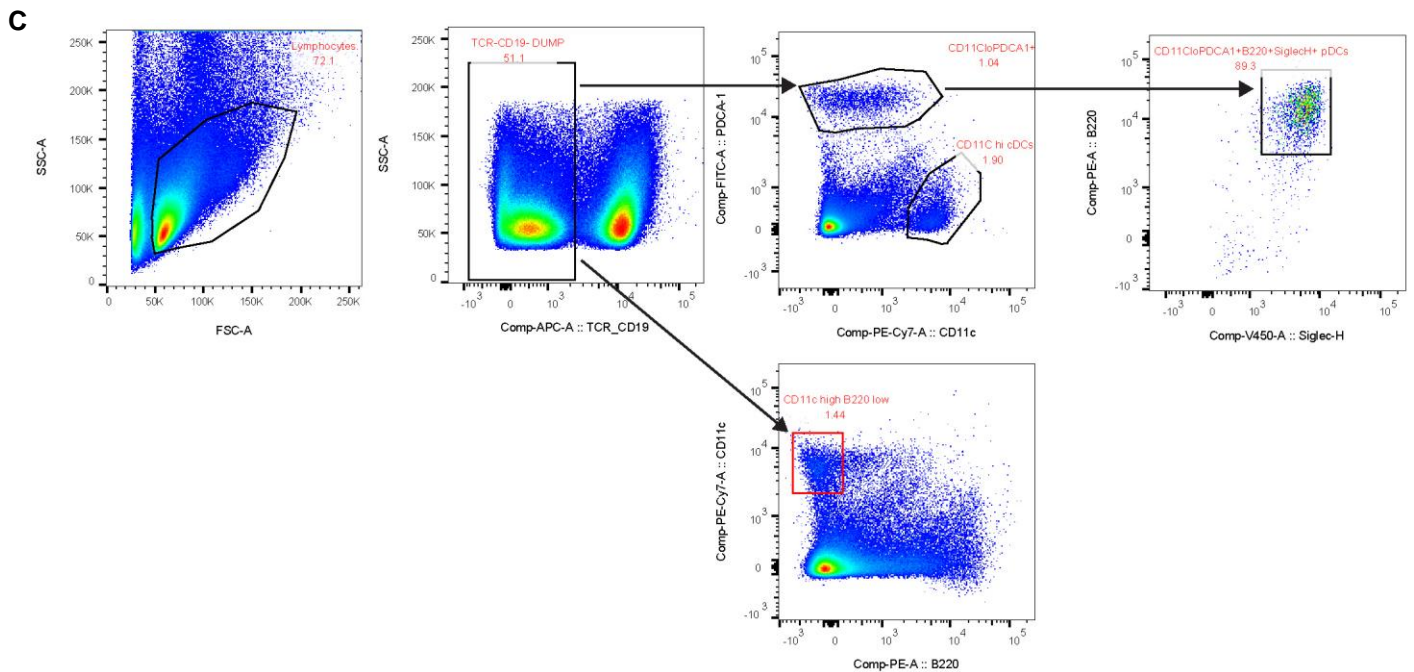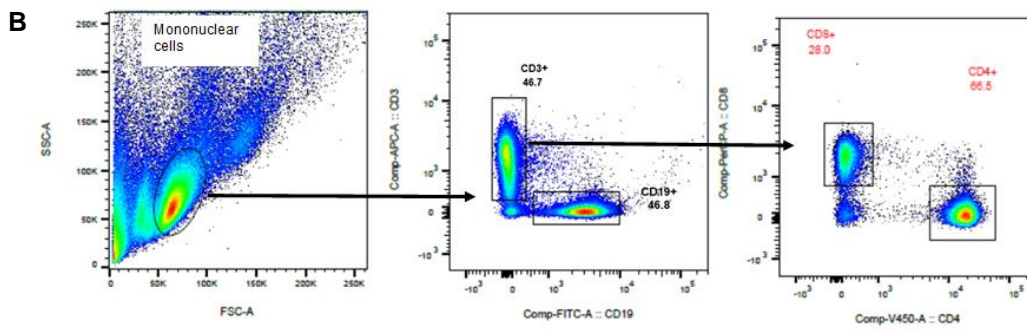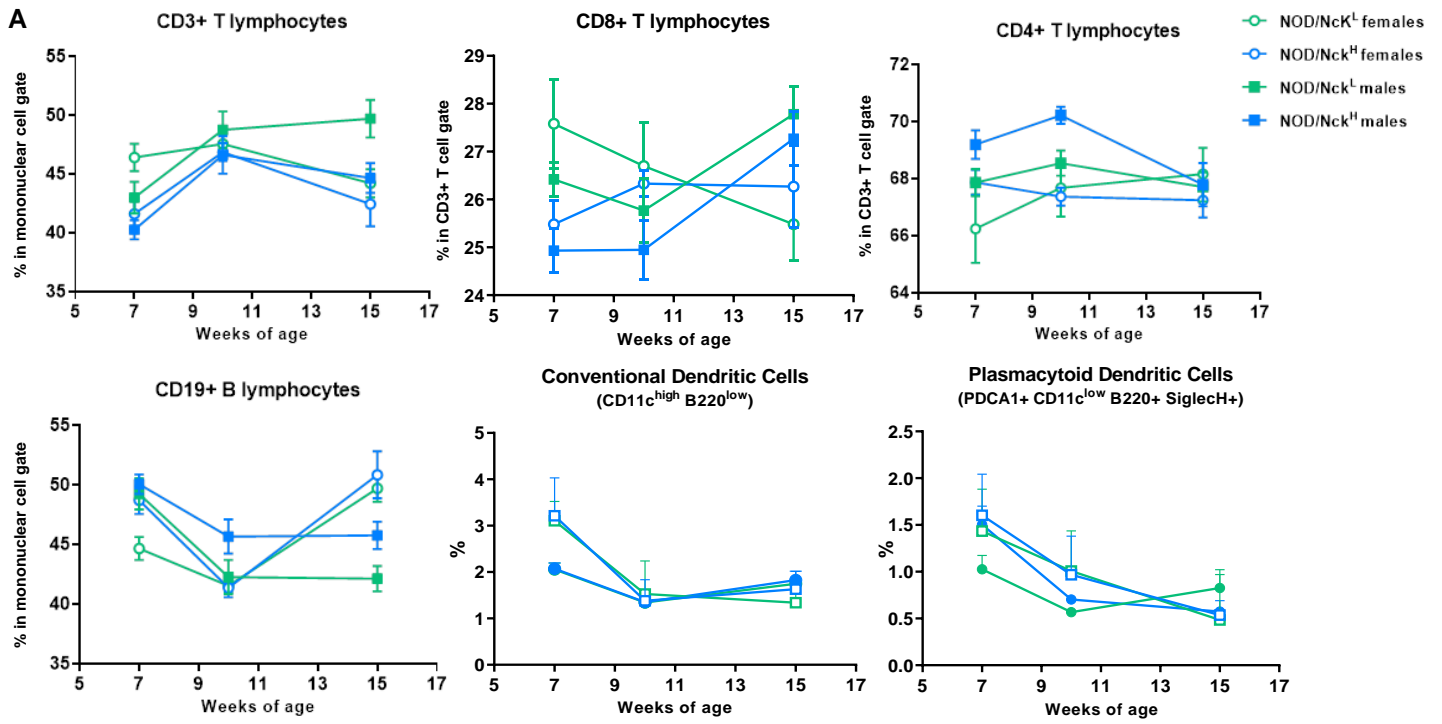DSP_MapKP   DSP_DUSP10

Fig. S2.

Dusp10 nucleotide sequence and deduced amino acid sequence. This diagram shows the part of the first *Dusp10* domain containing the nonsynonymous G to T transversion resulting in the cysteine-to-phenylalanine missense mutation at position 73 in the protein DUSP10 (black square) in NOD/Nck^H mice. The mutation in CR#13 mice is also shown, here the deletion of a single nucleotide generates a premature STOP codon at position 86 of the protein (red square). Amino acid numbers are shown above. The variant we describe here is localized in the possibly intrinsically disordered first N-terminal domain (from residue 1 to 143, as predicted by Spot-Disorder, alternation of ordered and disordered regions from residue 1 to predicted 140 by PrDos and from residue 1 to 155 by Biomine).

Fig. S3.

Alignment of putative orthologues of the murine (*Mm*) and human (*Hs*) Dusp10 protein in representative vertebrates. *Crp: Crocodylus porosus,* reptile, crocodile; *Chp*: *Chrysemys_picta_bellii* reptile*,* turtle (sub- class chelonia); *Gg:Gallus gallus* Aves; *Xt*: *Xenopus tropicali*s, amphibia; *Rt: Rhincodon typus* Chondrichthyes (cartilaginous fishes) Whale shark; *Dr*: *Danio rerio*, Actinopterygii (sub- class bony fishes); *Pm: Petromyzon marinus* Hyperoartia, Sea Lamprey. The red symbol indicates the Cys to Phe mutation of the mouse Dusp10 protein discussed in the text. Alignment carried out with MAFFT G-INS-i with default parameters and visualised with BoxShade. Double headed arrows: Orange: intrinsically disordered sequence, Blue: central "Rhodanese-like" domain, Green: catalytic domain.

A

CD3+ T lymphocytes

CD8+ T lymphocytes

CD4+ T lymphocytes

○ NOD/NcK^L females
○ NOD/NcK^H females
■ NOD/NcK^L males
■ NOD/NcK^H males

CD19+ B lymphocytes

Conventional Dendritic Cells
(CD11c^high B220^low)

Plasmacytoid Dendritic Cells
(PDCA1+ CD11c^low B220+ SiglecH+)

B

C

Fig. S4.

Immune cell subsets in the spleen of NOD/Nck^H and NOD/Nck^L at different ages. (**A**) Immune cell subsets were monitored in the spleen of NOD/Nck^H and NOD/Nck^L mice at different ages using flow cytometry. Data are presented as means ± SEM of 6 individuals analyzed at each point in time. No significant differences were observed when comparing at the same age values observed between the two different sublines and also considering the different genders. (**B-C**) Flow cytometry gating strategies for T cells and B cells (**B**) or conventional dendritic cells and plasmacytoid dendritic cells (**C**).
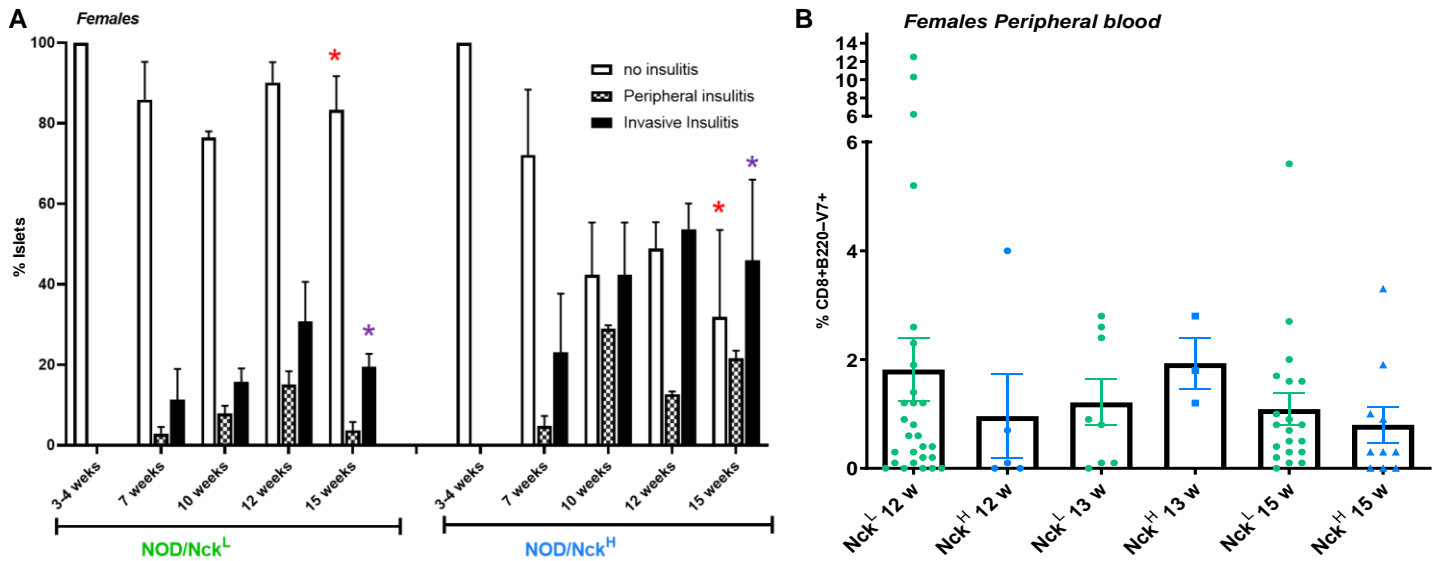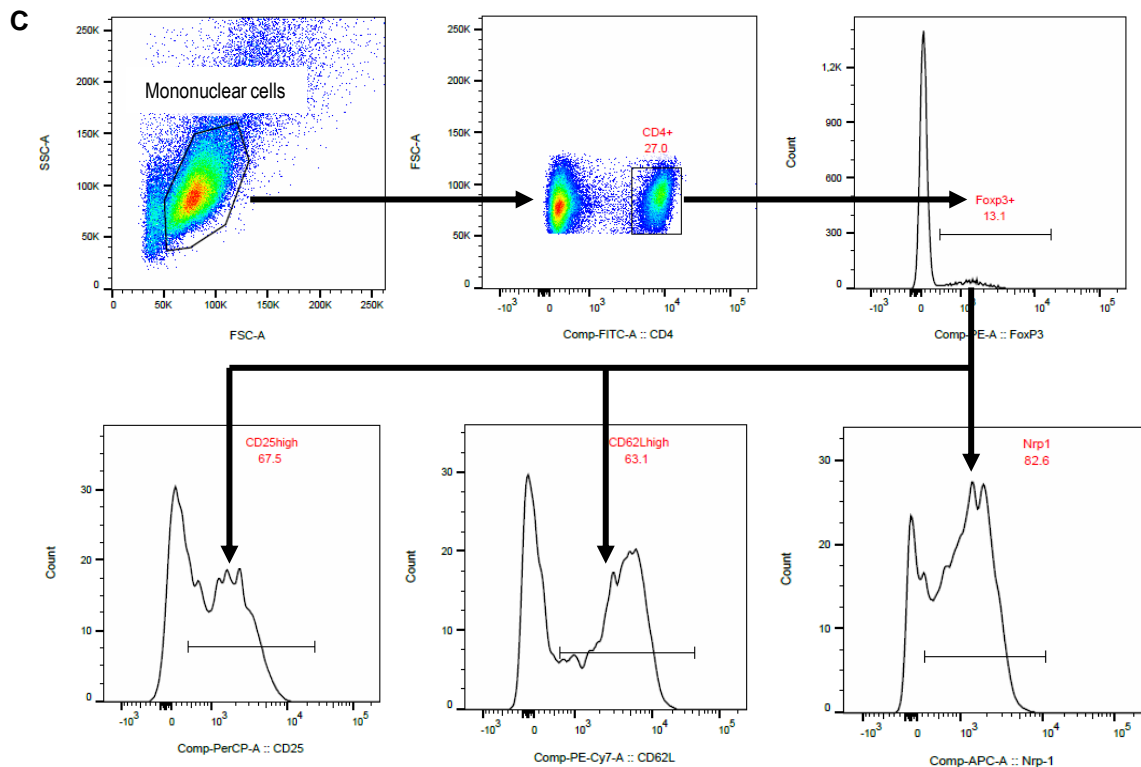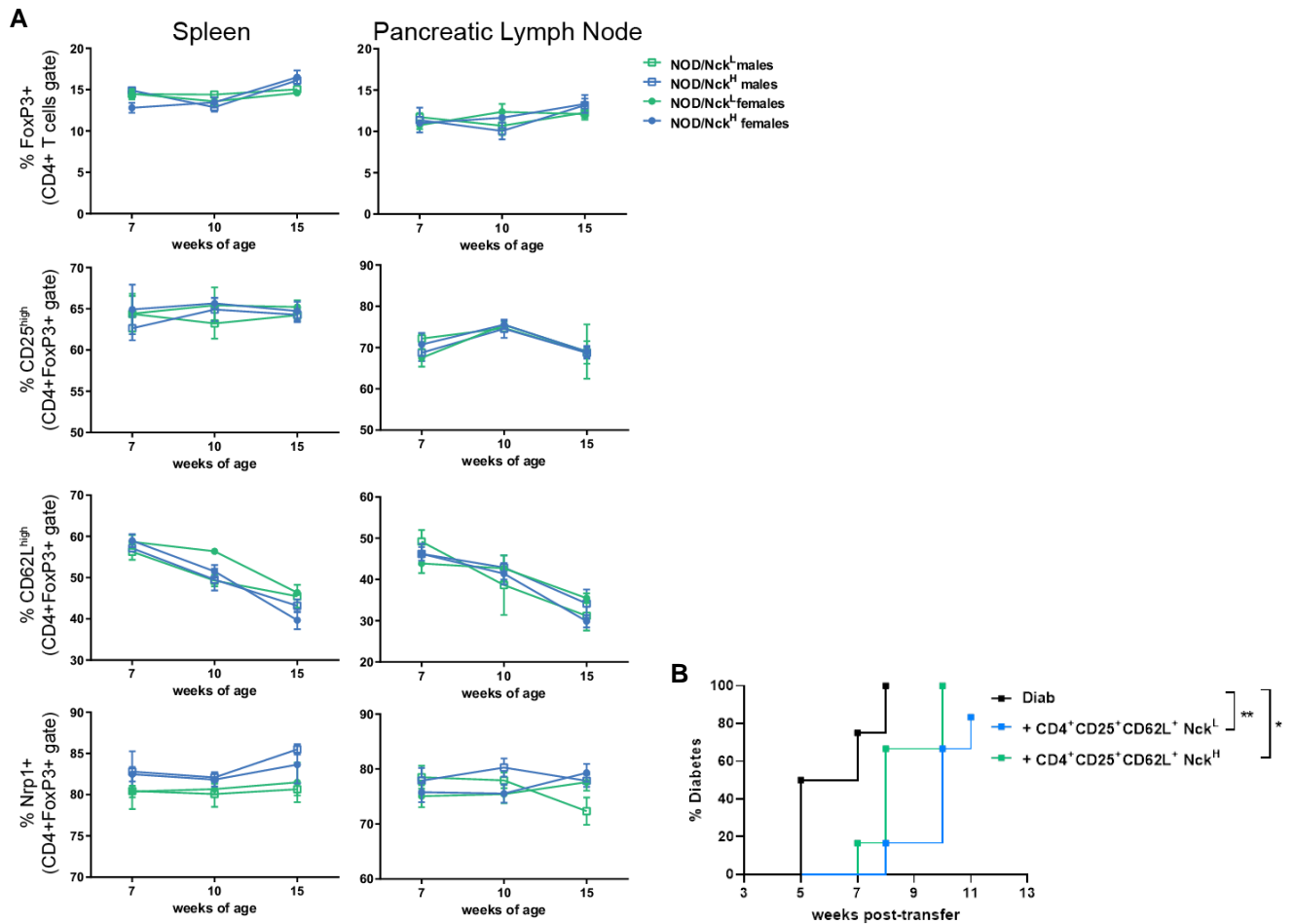
Fig. S5.

Islet infiltration and pathogenic T lymphocytes in female NOD/Nck[H] and NOD/Nck[L]. (**A**) Insulitis was monitored in NOD/Nck[H] and NOD/Nck[L] female mice as described in legend of figure 2; 60 to 100 islets were counted per pancreas from 3-6 individuals. Results are expressed as mean ± SEM. At 15wks of age in NOD/Nck[H] mice a significant decrease (red asterisk) in the proportion of normal non-infiltrated islets and a significant increase (black asterisk) of islets with invasive insulitis was observed as compared to NOD/Nck[L] (Mann Whitney test, p<0.0094 and p<0.0029 respectively). (**B**) Pathogenic CD8+ T cells specific for the beta-cell-specific IGRP$_{206-214}$ epitope were enumerated in peripheral blood of NOD/Nck[H] and NOD/Nck[L] male mice using the NRP-V7 mimotope as previously described (1). Data are expressed in individual mice as % NRP-V7+ cells within the CD8+B220- gate and also presented as mean ± SEM of the analyzed individuals.
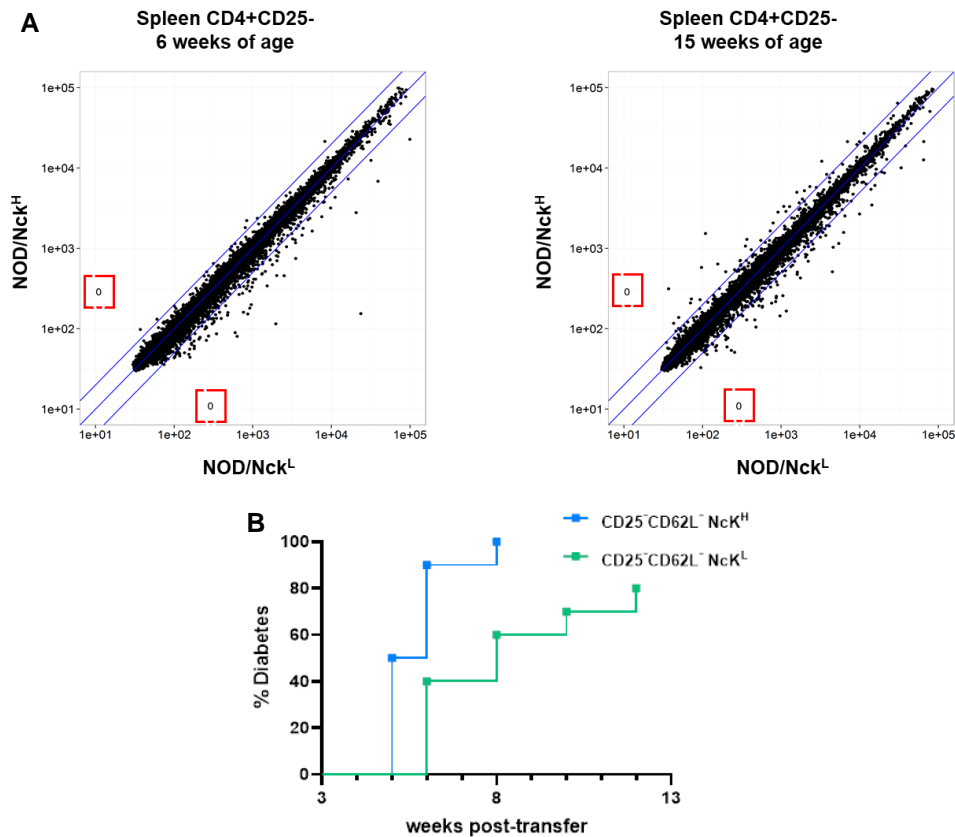
Fig. S6.

Analysis of pathogenic CD4+ T cells in NOD/Nck sublines. (**A**) Transcriptome-wide expression scatter plot of average gene expression in NOD/Nck[H] and NOD/Nck[L] mice of male spleen CD4+CD25- T cells recovered at 6 and 15 weeks of age. This population is depleted of regulatory T cells (CD4+CD25+FoxP3+) **(2-6)** and is enriched in CD4+ pathogenic lymphocytes (CD4+CD62L-) **(7)**. Confronting these samples, no genes were significantly up or down regulated (Fold change > 1.5 and FDR<0.05), as indicated by the numbers in the red boxes. (**B**) Splenocytes were recovered from 10 wk-old NOD/Nck[H] and NOD/Nck[L] male donors. Cells were purified by magnetic cell sorting (MACS) to recover CD25-CD62L- T cells (CD4+ and CD8+), a population depleted of regulatory T cells and enriched in pathogenic cells (2-7). As previously shown this population is highly effective at transferring autoimmune diabetes in immunoincompetent recipients (as effective as total spleen cells from overtly diabetic donors (4)). NOD/Nck $Rag^{-/-}$ recipients were adoptively transferred with 0.4×10^6 purified CD25-CD62L- T cells from NOD/Nck[H] or NOD/Nck[L] mice. Incidence of diabetes was monitored in recipients (n=10/group). Transfer of disease was very effective with the two cell populations tested. Actuarial survival curves were compared using the Logrank (Mantel-Cox) statistical test. The difference observed is significant (p=0.0025) and well reflects the time-shifted difference in the advent of autoimmune diabetes observed in NOD/Nck[H] as compared to NOD/Nck[L] mice.

A

Spleen

Pancreatic Lymph Node

Legend:
- NOD/Nck^L males
- NOD/Nck^H males
- NOD/Nck^L females
- NOD/Nck^H females

Y-axes (Spleen and PLN columns):
- % FoxP3+ (CD4+ T cells gate)
- % CD25^high (CD4+FoxP3+ gate)
- % CD62L^high (CD4+FoxP3+ gate)
- % Nrp1+ (CD4+FoxP3+ gate)

X-axis: weeks of age

B

Legend:
- Diab
- + CD4$^+$CD25$^+$CD62L$^+$ Nck^L
- + CD4$^+$CD25$^+$CD62L$^+$ Nck^H

** *

Y-axis: % Diabetes
X-axis: weeks post-transfer

C

Mononuclear cells

CD4+ 27.0

Foxp3+ 13.1

CD25high 67.5

CD62Lhigh 63.1

Nrp1 82.6

Fig. S7.

Analysis of regulatory CD4+ T cells in NOD/Nck sublines. (**A**) Phenotypic analysis by flow cytometry of regulatory T cells in the spleen and pancreatic lymph nodes of male and female NOD/Nck^H and NOD/Nck^L mice at 7, 10 and 15 weeks of age. The figure details the proportions in each lymphoid organ of FoxP3+ cells in the CD4+ T cells gate and of CD4+CD25^{high}, CD62L^{high} and (Neuropilin 1) Nrp+ cells in the CD4+FoxP3+ gate. Data are presented as means ± SEM of 6 individuals analyzed at each point in time. No significant differences were observed when comparing at the same age values observed between the two different sublines and also considering the different genders. (**B**) Adoptive co-transfer in NOD/Nck *Rag* $^{-/-}$ recipients of a mixture of 3 x 10^6 diabetogenic cells (total spleen cells from overtly diabetic mice) and 3 x 10^6 of magnetic sorted CD4+CD25^{high}CD62L^{high} cells, a population highly enriched in regulatory T cells (2-6), from 14-week-old NOD/Nck^H or NOD/Nck^L. Controls were injected with diabetogenic T cells alone. Actuarial survival curves were compared using the Logrank (Mantel-Cox) statistical test. Disease transfer by diabetogenic cells was significantly delayed by regulatory T cells from both NOD/Nck^H (p=0.039) and NOD/Nck^L (p=0.0032). (**C**) Flow cytometry gating strategies for subsets of CD4+FoxP3+ regulatory T cells.
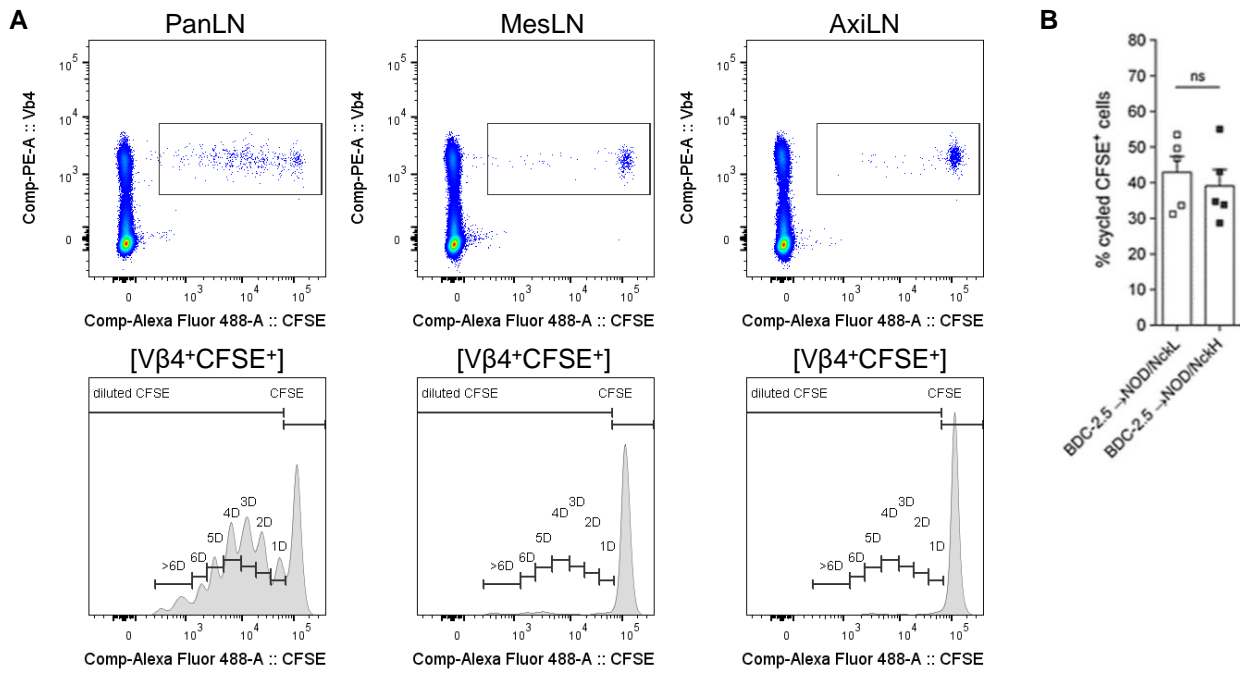
Fig. S8.

Timing of islet antigens presentation in NOD/Nck sublines. Similar timing of islet antigen presentation was observed in NOD/Nck[H] and NOD/Nck[L] mice as assessed by a well- established method (8). (**A**) NOD/Nck[H] and NOD/Nck[L] mice were injected i.v at 4 weeks of age with 1x106 CFSE-labelled transgenic BDC-2.5 CD4+ T cells (Vbeta 4[+]) expressing a T cell receptor specific for an insulin-chromogranin A fusion peptide (9). Proliferation of transferred cells in was analyzed by flow cytometry 96 hours after injection in pancreatic draining lymph nodes (PanLN) as compared to mesenteric lymph nodes (MesLN) and axillary lymph nodes (AxiLN) of recipient mice. As already described BDC-2.5 CD4+ T cells proliferated exclusively in pancreatic lymph nodes where the cognate islet antigens is presented (8). (**B**) An identical capacity of diabetogenic cells expressing the transgenic BDC2.5 T cell receptor to migrate and proliferate in pancreatic lymph-nodes when adoptively transferred into 4-week-old recipients. Results are expressed as the percentage of CFSE proliferating cells in mice of the two sublines of 106 CFSE-labelled naïve BDC-2.5 CD4+ T cells. Mann-Whitney test; ns, non-significantly different.

12
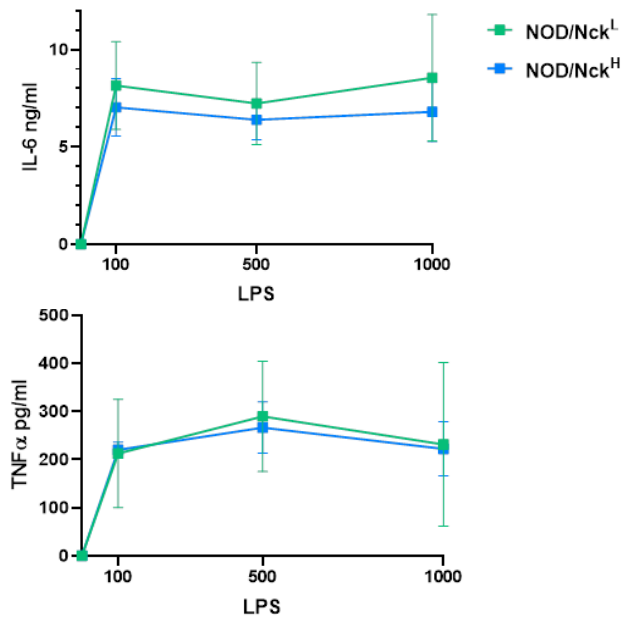
Fig. S9.

Innate immune response in NOD/Nck^H and NOD/Nck^L mice. IL-6 and TNFα production by peritoneal macrophages of NOD/Nck^H and NOD/Nck^L mice (male mice, 8-10 weeks of age) upon lipopolysaccharide (LPS) stimulation. No significant differences were observed.

Table S1.

Coding SNPs and Small Indels specific for the NOD/NckL and NOD/NckH sublines.

Chr	Position	Reference	Variant	Type	Class	Subline	Gene Name	Amino acid change	*Idd* region
chr1	20914658	G	T	Intragenic		NOD/Nck^L	*Paqr8*	-	*Idd26*
chr1	153744230	G	A	3' UTR		NOD/Nck^H	*Rgs16*	-	*Idd5.4b*
chr1	184037056	G	T	Non-synonymous	Missense	NOD/Nck^H	*Dusp10*	C73F	-
chr1	36533553			3' UTR		NOD/Nck^L	*Gm5615* *	-	*Idd2*
chr4	149952486	C	T	Intragenic		NOD/Nck^L	*Spsb1*	-	*Idd9.3*
chr5	31487373	GAGAAG	GAG	Codon deletion		NOD/Nck^L	*4930548H24Rik*	-	-
chr7	30878082	C	T	Non-synonymous	Missense	NOD/Nck^L	*Cd22*	R2H	-
chr7	87243067	A	G	Intragenic		NOD/Nck^L	*Nox4*	-	*Idd27*
chr8	119633519	G	T	Stop gained	Nonsense	NOD/Nck^H	*Kcng4*	Y39*	-
chr8	122495569	G	A	Non-synonymous	Missense	NOD/Nck^H	*Fam38a (Piezo1)*	R941W	-
chr9	20438546	C	A	Non-synonymous	Missense	NOD/Nck^H	*Zfp26*	A241S	-
chr13	64287285	G	A	Intragenic		NOD/Nck^L	*Aaed1*	-	*Idd14*
chr14	20469411	C	T	Non-synonymous	Missense	NOD/Nck^H	*Anxa7*	G113E	-
chr15	35846957	G	T	Non-synonymous	Missense	NOD/Nck^H	*Vps13b*	A2629S	-
chr17	35380405	G	A	Non-synonymous	Missense	NOD/Nck^L	*H2-Q4*	*D155N*	*Idd24*
chrX	7560336	C	A	Non-synonymous	Missense	NOD/Nck^H	*Ppp1r3f* *	G562V	-

Dataset S1. (separate file)

Validated DNA sequence variants distinguishing NOD/Nck^H and NOD/Nck^L sublines used for Automated Meiotic Mapping.

References

1. Trudeau JD, et al., Prediction of spontaneous autoimmune diabetes in NOD mice by quantification of autoreactive T cells in peripheral blood. *The Journal of clinical investigation* **111**:217-223 (2003).
2. Alyanakian MA, et al., Diversity of regulatory CD4+T cells controlling distinct organ-specific autoimmune diseases. *Proceedings of the National Academy of Sciences of the United States of America* **100**:15806-15811 (2003).
3. Salomon B, et al., B7/CD28 costimulation is essential for the homeostasis of the CD4+CD25+ immunoregulatory T cells that control autoimmune diabetes. *Immunity* **12**:431-440 (2000).
4. You S, et al., Autoimmune diabetes onset results from qualitative rather than quantitative age-dependent changes in pathogenic T-cells. *Diabetes* **54**:1415-1422 (2005).
5. You S, et al., Adaptive TGF-beta-dependent regulatory T cells control autoimmune diabetes and are a privileged target of anti-CD3 antibody treatment. *Proceedings of the National Academy of Sciences of the United States of America* **104**:6335-6340 (2007).
6. You S, et al., Unique role of CD4+CD62L+ regulatory T cells in the control of autoimmune diabetes in T cell receptor transgenic mice. *Proceedings of the National Academy of Sciences of the United States of America* **101 Suppl 2**:14580-14585 (2004).
7. Lepault F Gagnerault MC, Characterization of peripheral regulatory CD4+ T cells that prevent diabetes onset in nonobese diabetic mice. *Journal of immunology (Baltimore, Md. : 1950)* **164**:240-247 (2000).
8. Höglund P, et al., Initiation of autoimmune diabetes by developmentally regulated presentation of islet cell antigens in the pancreatic lymph nodes. *The Journal of experimental medicine* **189**:331-339 (1999).
9. Delong T, et al., Pathogenic CD4 T cells in type 1 diabetes recognize epitopes formed by peptide fusion. *Science (New York, N.Y.)* **351**:711-714 (2016).